Quantifying Chemical Tagging: Towards Robust Group Finding in the Galaxy

A. W. Mitschang[1,2] $\star$, G. De Silva[3], S. Sharma[4], D. B. Zucker[1,2,3]

[1] *Macquarie University Research Centre in Astronomy, Astrophysics & Astrophotonics, NSW 2109, Australia*
[2] *Department of Physics & Astronomy, Macquarie University, NSW 2109, Australia*
[3] *Australian Astronomical Observatory, PO Box 915, North Ryde, NSW 1670, Australia*
[4] *Sydney Institute for Astronomy, School of Physics, University of Sydney, NSW 2006, Australia*

10 September 2021

ABSTRACT

The first generation of large-scale chemical tagging surveys, in particular the HER-MES/GALAH million star survey, promises to vastly expand our understanding of the chemical and dynamical evolution of the Galaxy. This, however, is contingent on our ability to confidently perform chemical tagging on such a large data-set. Chemical homogeneity has been observed across a range of elements within several Galactic open clusters, yet the level to which this is the case globally, and particularly in comparison to the scatter across clusters themselves, is not well understood. The patterns of elements in coeval cluster members, occupying a complex chemical abundance space, are rooted in the evolution, ultimately the nature of the very late stages, of early generations of stars. The current astrophysical models of such stages are not yet sufficient to explain all observations, combining with our significant gaps in the understanding of star formation, makes this a difficult arena to tackle theoretically. Here, we describe a robust pair-wise metric used to gauge the chemical difference between two stellar components. This metric is then applied to a database of high-resolution literature abundance sources to derive a function describing the probability that two stars are of common evolutionary origin. With this cluster probability function, it will be possible to report a confidence, grounded in empirical observational evidence, with which clusters are detected, independent of the group finding methods. This formulation is also used to probe the role of chemical dimensionality, and that of individual chemical species, on the ability of chemical tagging to differentiate coeval groups of stars.

Key words: stars: abundances – Galaxy: open clusters and associations: general – techniques: miscellaneous (chemical tagging) – methods: statistical

1 INTRODUCTION

It has long been postulated that stars form in dense clusters out of an overdensity of primordial gas and dust (e.g. see Shu et al. 1987). Evidence for this is seen in present day open clusters, but their numbers by no means account for the large stellar population of the Galactic disk. Janes et al. (1988) suggest that a typical lifetime of an open cluster in the disk is 100 Myr, after which their stellar components dissipate through dynamical interactions, explaining the fact that stars are not strictly observed in clusters. It is possible this dissipative action is seen in progress in so-called "moving groups" and young associations (e.g. Eggen 1994; Montes et al. 2001; Zuckerman & Song 2004; Torres et al. 2008). A small but significant population of very old open clusters have since been identified (Phelps et al., 1994; Janes & Phelps, 1994;

Friel, 1995), notably including NGC 6791 with an age of ~7.2 Gyr (Kaluzny & Rucinski, 1995), with the zone in-between filled by a wide range of ages (Xin & Deng, 2005). Present day star formation within embedded molecular clouds, such as the Orion nebula, completes the circle of cluster evolution (Lada & Lada, 2003). These observations indicate that stars indeed have formed and continue to form in clusters through all epochs of Galactic evolution.

Although the particulars of star formation in molecular clouds remain uncertain, the observed abundances of elements point to a successive chain of star formation, chemical enrichment of the interstellar medium, and subsequent formation events in a cloud, occurring over generations of stars. Most of the elements known to exist in the universe are processed in the very late stages or death throes of a star (e.g. see Wallerstein et al. 1997). The origin of the Fe-peak elements is believed to be primarily in type Ia supernovae, while the α-, and r-process elements are most likely predominantly generated within the violent explosions of core-

$\star$ E-mail: arik.mitschang@mq.edu.au

collapse (type II) supernovae (Kratz et al., 2007). The relatively more quiescent asymptotic giant branch (AGB) phase, in low- to intermediate-mass stars, is thought to be responsible for most of the s-processing (Karakas & Lattanzio, 2007; Busso et al., 1999), and thus is the sole origin of the pure s-process elements and a contributor of elements produced by both the s- and r-processes. The next generation of low mass stars, born out of this freshly enriched gas and dust cloud, will spend a significant amount of time on the main sequence and giant branches. In these stages, and at these masses, the nuclear processing and convection fueling the star are not sufficient to alter the photospheric abundances of those elements (Iben, 1967). Therefore, it is these groups of elements that form the basis of the technique that has come to be known as chemical tagging.

The technique of chemical tagging, first proposed by Freeman & Bland-Hawthorn (2002), promises to identify clusters of stars, even after being scattered by the dissipative evolution of the disk, through patterns of abundances in these key elements. To date, several important test have been made, confirming that members of individual open clusters are chemically homogeneous (De Silva et al., 2009, 2007a), as well as less obvious kinematically linked stellar aggregates known as moving groups (De Silva et al., 2007b; Bubar & King, 2010). The technique has not, to our knowledge, been applied on any scale to a random sample of stars, but has been utilized to confirm or reject suspected membership amongst kinematic groups in several recent studies (e.g. Tabernero et al. 2012; Pompéia et al. 2011; Carretta et al. 2012; De Silva et al. 2011). A particular challenge is the large number of dimensions that are required in order to guarantee uniqueness across populations; Bland-Hawthorn & Freeman (2004) and De Silva et al. (2007a) estimate between 10 and 15 elements, are necessary, given the number of formation sites and some assumptions of abundance accuracy. These elements form the dimensions of the so-called $\mathcal{C}$-space (Freeman & Bland-Hawthorn, 2002). The sample size of studies with sufficient abundances, however, remains small.

The ambitious chemical tagging project known as the GALactic Archaeology with HERMES (GALAH[1]) survey, to be undertaken with the upcoming High Efficiency and Resolution Multi-Element Spectrograph (HERMES;Barden et al. 2010), will target a million disk stars at high-resolution in a relatively short time-span. The possibility of piecing back together some of the presumably 10^8 relic clusters dissolved in the Galaxy (Bland-Hawthorn & Freeman, 2004), could vastly expand our knowledge of the star formation history and structural and chemical evolution of the Galactic disk. The Gaia-ESO Public Spectroscopic Survey (Gilmore et al., 2012), an on-going chemical abundance analysis survey, will target approximately 100000 field and open cluster stars in the Galaxy at high resolution, providing a rich dataset complementing GALAH. A very interesting prospect is the search for Solar siblings, or the birth cluster of the Sun, and its origin and possible journey within the Galaxy (Bland-Hawthorn et al., 2010b; Batista & Fernandes, 2012). The ability to tackle these arenas is dependent on the ability to reliably distinguish compatible from incompatible chemistries (i.e. between two stars in such a survey).

We present here, for the first time, a metric that quantifies, in a consistent yet flexible manner, global abundance trends in terms of chemical tagging and show how a given population can be probed using this metric, along with a representative cluster sample, without the need to define an arbitrary "level" of chemical homogeneity. We show how any stellar population can be chemically tagged, and how a quantitative level of confidence can be applied to its members to gauge the overall quality of a detection based solely on elemental abundances. We further discuss some implications of this approach to carrying out large scale chemical tagging surveys such as GALAH.

2   A METRIC TO PROBE THE CHEMICAL NATURE OF CLUSTERS

On the subject of chemical tagging, there has been little discussion in the literature thus far on establishing *quantitative* differences in chemical signatures between different clusters and the stars within a given cluster. Several authors have obtained and analyzed high resolution data-sets on known cluster or moving group populations with the aim of testing chemical tagging (De Silva et al., 2007a,b, 2009; Bubar & King, 2010) with quite promising results. These studies have taken a qualitative approach to differences in chemical abundance patters. There has also been work recently on understanding the complexity and interrelation of the chemical abundance space using Principle Component Analysis (Ting et al., 2012). The goal there is to reduce the overall dimensionality to only the strongest variant dimensions. That study, however, was restricted to probing the chemical patterns *between* different populations, including open clusters, looking for the largest scatter in nucleosynthesis yields. There is still lacking a global characterization of the differences in patterns in $\mathcal{C}$-space, e.g. the level of homogeneity expected within a cluster is not clearly defined.

The difficulty in conceptualizing the interplay between all of the dimensions of $\mathcal{C}$-space, combined with the non-uniformity of the available abundance data, leads us to seek a description of the chemical difference between clusters that is both independent of the dimensionality of $\mathcal{C}$-space, and itself one-dimensional.

2.1   A metric for determining chemical difference

We define a simple metric for quantifying the chemical difference between any two stars

$$\delta_C = \sum_C^{N_C} \omega_C \frac{|A_C^i - A_C^j|}{N_C}$$

Where C is a particular chemical species out of the N_C species for which abundances have been determined, A_C is the abundance ratio of element C to Fe relative to solar (i.e. [X/Fe] in standard notation), except when C is Fe, in which case it is the ratio of Fe to H; i and j are the two stars for which this metric is being computed; and ω_C represents a weighting factor for an individual species. For this work, ω_C is always equal to one, but is included in this definition for future investigations, when sufficiently large data-sets, which will allow its examination, become available. Simply put, δ_C is the mean absolute difference of species C between two stars across all N_C chemical species. There are two reasons for the choice of this type of metric (a Manhattan type) as opposed to a Euclidean type. First and foremost, its use facilitates the separation of clusters in $\mathcal{C}$-space, the ultimate goal of chemical tagging, and secondly, the value of δ_C is more easily interpreted in the context of abundance measurements. Another advantageous property of this metric definition, due to the N_C denominator, is that when considering any

number of correlated elements in the summation, the value of δ_C is independent of the number of number of elements, N_C.

In this paper, the binned probability density distribution of δ_C for a single population, normalized to its maximum per-bin δ_C number density, shall be referred to as the η_C distribution. When such a population contains only members of a cluster, i.e. a single group of coeval stars, chemical tagging theory posits that this distribution should occupy the low end of the difference spectrum, while populations derived from strictly distinct clusters will occupy the high end. The following two terms describe these different populations and will be used throughout this text. Their definitions and uses should be understood as follows:

• **intra-cluster**: All members of this group are confirmed members of a single open cluster. η_C will be built from those δ_C computed between any two stars that satisfy the above definition and for which any stated conditions apply (e.g. minimum number of elements, etc.)

• **inter-cluster**: Members of this group are confirmed members of any open cluster. η_C will be built from all those δ_C computed between two stars that are *not* members of the same open cluster and for which any stated conditions apply.

Figure 1 shows both intra- and inter-cluster η_C distributions for the clusters listed in Table 1, calculated with the condition that a minimum of 8 elements be used in the δ_C computation (for a detailed explanation of this choice, see section 5). We note that the total range of the inter-cluster distribution is much larger than that depicted, however it is not instructive to display anything beyond the range of the intra-cluster distribution for the purposes of our analysis. It is important also to note that, because we do not assume a cluster is represented by its mean abundances, the inter-cluster distribution takes into account all scatter within a given cluster, across all chemical dimensions. This point is crucial to our analysis, and its potential usefulness in terms of a true chemical tagging experiment, in that we wish to determine the ability to distinguish individual pairs of stars. Assuming perfect homogeneity amongst cluster members in this respect would likewise circumvent our treatment of the intra-cluster distribution.

2.2 Open cluster abundance data

Table 1 gives a summary of the literature elemental abundance database generated for use in this analysis. Each row in the table is a particular study, from the literature, of a single cluster as indicated. Basic information includes the cluster name, the number of stars for which abundances were derived ($N_\star$), the total number of element species derived (N_C), and the literature reference. The remaining columns in the table summarize the abundance data: for each element existing in the database, the number of stars for which abundances for that element were derived is listed. The numbers in this matrix are equal to or less than the corresponding $N_\star$, depending on, for example, the range or quality of a particular spectrum.

The table was generated first using sources listed in Table 12 of Carrera & Pancino (2011), and then by a literature search for any other studies based on high-resolution data for open clusters with abundances of those elements listed in Table 1. Due to the sensitivity of computed abundances, especially when derived from equivalent widths (EWs), with respect to resolution, and in order to best match upcoming chemical tagging surveys, we only considered studies whose typical resolution was better than R∼28,000. We also only considered individual clusters which had at least four stars for which abundances were derived. This latter condition is
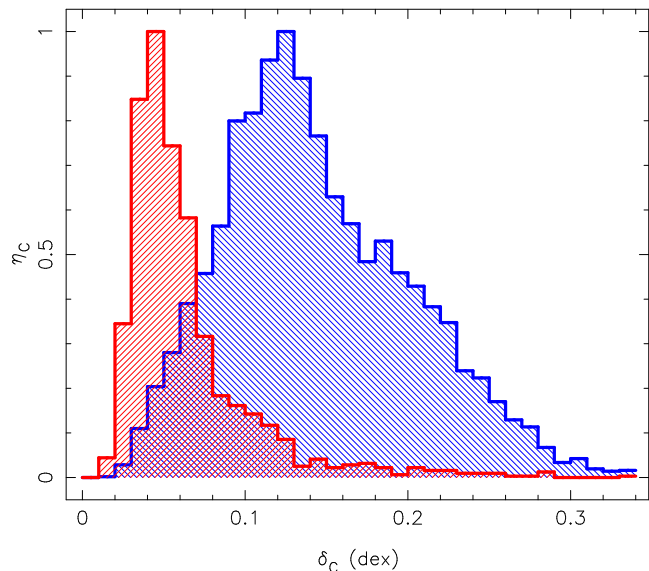

Figure 1. The η_C distributions for intra- (red; left) and inter-cluster (blue; right) populations. The total range of the inter-cluster distribution is larger than shown, and has been cut off as described in the text.

Table 2. Sources and designations used in Table 1

Source reference	Label
Soderblom et al. (2009)	A
D'Orazi & Randich (2009)	B
Ford et al. (2005)	C
Sestito et al. (2008)	D
Shen et al. (2005)	E
Bragaglia et al. (2008)	F
Pace et al. (2008)	G
Magrini et al. (2010)	H
De Silva et al. (2007a)	I
Randich et al. (2006)	J
Carretta et al. (2007)	K
Gonzalez & Wallerstein (2000)	L
Smiljanic et al. (2009)	M
De Silva et al. (2006); Paulson et al. (2003)	N
Carretta et al. (2005)	O
Pereira & Quireza (2010)	P
Mitschang et al. (2012)	Q
Gebran et al. (2008)	R
Gebran & Monier (2008)	S
Tautvaišiene et al. (2000)	T
Reddy et al. (2012)	U

an optimisation between the total number of clusters included and the number of pairs used for the intra-cluster distribution, ensuring adequate statistical significance for both populations. There proved to be no reason to limit the number of chemical species derived in a particular study (N_C); indeed the range allows us to probe some of the effects of chemical dimensionality on the technique of chemical tagging, which will be discussed in more detail in Section 5.

All abundance values collected in the database are with respect to Fe and compared to solar, i.e. [X/Fe] in standard notation. Fe abundances are the only exception and are tabulated as [Fe/H]. Where a literature study reported abundances otherwise, those values were converted to this system when possible, and otherwise omitted. Care was taken to ensure that the studies targeted

Table 1. Summary of the high-resolution literature abundance database

Cluster	Source[a]	$N_\star$	N_C	Na	Mg	Al	Si	Ca	Sc	Ti	V	Cr	Mn	Fe	Co	Ni	Cu	Zn	Sr	Y	Zr	Ba	La	Ce	Nd	Sm	Eu
Pleiades	A	20	5	20	-	-	20	-	-	20	-	-	-	20	-	20	-	-	-	-	-	-	-	-	-	-	-
IC2391	B	7	6	7	-	-	7	7	-	7	-	-	-	7	-	7	-	-	-	-	-	-	-	-	-	-	-
IC2602	B	8	6	8	-	-	8	8	-	8	-	-	-	8	-	8	-	-	-	-	-	-	-	-	-	-	-
Blanco1	C	8	6	-	8	-	8	8	-	8	-	-	-	8	-	8	-	-	-	-	-	-	-	-	-	-	-
Be29	D	6	6	-	-	-	6	6	-	6	-	6	-	-	-	6	-	-	-	-	-	6	-	-	-	-	-
Cr261	D	7	6	-	-	-	7	7	-	7	-	7	-	-	-	7	-	-	-	-	-	7	-	-	-	-	-
Mel66	D	6	6	-	-	-	6	6	-	6	-	6	-	-	-	6	-	-	-	-	-	6	-	-	-	-	-
IC4665	E	18	6	-	18	-	18	18	-	18	-	18	-	-	-	18	-	-	-	-	-	-	-	-	-	-	-
Be32	F	9	8	9	-	-	9	9	-	9	-	9	-	9	-	9	-	-	-	-	-	9	-	-	-	-	-
NGC2324	F	7	8	7	-	-	7	7	-	7	-	7	-	7	-	7	-	-	-	-	-	7	-	-	-	-	-
NGC2477	F	6	8	6	-	-	6	6	-	6	-	6	-	6	-	6	-	-	-	-	-	6	-	-	-	-	-
NGC2660	F	5	8	5	-	-	5	5	-	5	-	5	-	5	-	5	-	-	-	-	-	5	-	-	-	-	-
NGC3960	F	6	8	6	-	-	6	6	-	6	-	6	-	6	-	6	-	-	-	-	-	6	-	-	-	-	-
IC4651	G	5	8	5	-	5	5	5	-	5	-	5	-	5	-	5	-	-	-	-	-	-	-	-	-	-	-
M67	G	6	8	6	-	4	6	6	-	6	-	6	-	6	-	6	-	-	-	-	-	-	-	-	-	-	-
Praesepe	G	7	8	7	-	5	7	7	-	7	-	7	-	7	-	7	-	-	-	-	-	-	-	-	-	-	-
NGC6192	H	4	8	-	4	4	4	4	-	4	-	4	-	4	-	4	-	-	-	-	-	-	-	-	-	-	-
NGC6404	H	4	8	-	4	4	4	4	-	4	-	4	-	4	-	4	-	-	-	-	-	-	-	-	-	-	-
Cr261	I	12	9	12	12	-	12	12	-	-	-	-	12	12	-	12	-	-	-	-	12	12	-	-	-	-	-
M67	J	10	9	10	10	10	10	10	-	10	-	10	-	10	-	10	-	-	-	-	-	-	-	-	-	-	-
NGC3532	M	5	9	-	5	-	5	5	5	5	5	5	-	-	5	5	-	-	-	-	-	-	-	-	-	-	-
NGC4756	M	5	9	-	5	-	5	5	5	5	5	5	-	-	5	5	-	-	-	-	-	-	-	-	-	-	-
NGC5822	M	5	9	-	3	-	5	5	5	5	5	5	-	-	5	5	-	-	-	-	-	-	-	-	-	-	-
NGC6791	K	4	9	-	4	4	4	4	4	4	-	-	4	-	-	4	-	-	-	-	-	4	-	-	-	-	-
M11	L	4	10	4	-	4	4	4	4	4	-	-	-	-	3	4	-	-	-	-	-	-	4	-	-	-	4
NGC6253	K	4	10	4	4	4	4	4	4	-	-	-	4	-	-	4	-	-	-	-	-	-	4	-	-	-	4
Hyades	N	46	12	46	46	-	46	46	-	46	-	-	-	46	-	-	-	46	-	-	46	46	18	46	46	-	-
Cr261	O	6	13	6	6	6	6	6	6	6	-	6	6	6	6	6	-	-	-	-	-	6	-	-	-	-	-
NGC3114	P	7	13	-	5	6	7	7	7	7	-	7	-	-	-	7	-	-	5	6	-	7	6	6	-	-	-
NGC3680	Q	11	14	11	11	8	11	11	-	11	-	11	-	11	-	11	-	11	-	11	-	8	7	-	8	-	-
Berenice	R	11	15	10	11	-	6	-	6	11	11	10	10	11	11	11	-	-	6	6	11	11	-	-	-	-	-
Pleiades	S	5	16	5	5	-	5	5	5	5	5	5	5	5	5	5	-	-	5	5	5	5	-	-	-	-	-
M67	T	9	20	9	9	9	9	9	9	9	9	9	9	9	9	9	9	-	-	9	9	9	9	9	-	-	9
NGC2360	U	4	21	4	4	4	4	4	4	4	4	4	3	4	4	4	4	2	-	4	4	3	3	2	-	3	-
NGC752	U	4	23	4	4	4	4	4	4	4	4	4	4	4	4	4	4	3	-	4	4	4	4	4	4	3	4

[a] References using designations listed in Table 2

Table 3. Literature abundance database columns format [†]

Cluster	CID	Star	SID	Src[a]	El	[X/Fe][b]	Error
NGC2360	50	12	1046	U	Al	-0.01	0.05
NGC2360	50	12	1046	U	Ca	0.13	0.06
NGC2360	50	12	1046	U	Co	0.03	0.09
NGC2360	50	12	1046	U	Cr	0.02	0.05
NGC2360	50	12	1046	U	Cu	-0.13	
⋮	⋱						

[†] The complete table with a detailed description of its contents is available in the electronic version of this text.
[a] As in Table 2
[b] Except for Fe → [Fe/H]

unevolved stars. Uncertainties, where available, are included in the database and are used to inform typical values as discussed later in the text.

The final database with individual abundances, which is available as a machine readable table with the online version of this text and on the web[2], contains 35 individual cluster studies of a total of 30 distinct clusters (clusters from separate studies are listed separately in Table 1) from 22 literature sources (those listed in Table 2). There are a total of 2775 individual abundance values measured for 291 stars, with a minimum and maximum chemical dimensionality of 5 and 23, respectively. A stub of the database is given in Table 3, where CID is a unique identifier for a given cluster in a given study, and SID is a unique identifier for a given star. These identifiers make it simple to disambiguate stars with repeated names and clusters from different studies. The complete version of Table 3 is available both online and in the electronic version of this paper. The tabulated abundance values from the literature were parsed via a computer program insofar as possible, and by hand in some cases where the formats were not as uniform. In very rare cases a literature study that matched our criteria may have proved to be too difficult to parse and load (e.g. a scanned hard copy) and had to be omitted.

2.3 The intra- and inter-cluster η_C distributions

Upon inspection of Figure 1 it is evident that the two populations have peaks significantly separated in δ_C space. Each peak can be thought of as the "characteristic" chemical difference of that population. In other words, based on Figure 1, we find that Galactic open clusters, as represented by our literature abundance database, typically differ chemically by ∼0.120 dex, while open clusters' *internal* scatter is typically at the ∼0.045 dex level. Next we draw the readers attention to the crossing point of the two distributions at ∼0.07 dex. This represents the point at which a pair of stars would be equally likely to inhabit the same cluster as they would to be members of entirely different clusters. Pairs of stars whose δ_C computes to the right of this line are then more likely than not to be of distinct origin, while those whose δ_C computes to the left would be considered more likely to be siblings.

Another obvious feature is the bump in inter-cluster η_C close to 0.19 dex. This is most likely due to noise on account of the limited numbers of clusters in this work and would smoothe out if more data were available. The extended tail toward high δ_C in the

[2] Note: To be uploaded to Vizier

intra-cluster distribution may also be attributed to noise, perhaps in the form of mis-identified group members. Another possible explanation for these "outliers" is related to errors in their abundance measurements. If not a noise feature, it may represent some form of cloud fragmentation in the progenitor of those clusters, giving rise to multi-modal star formation efficiencies within the same molecular cloud. In any case, as we shall demonstrate, neither of these features affects the probability analysis in the rest of this paper to any significant degree.

3 SYSTEMATICS

Systematic uncertainties folded into abundance determinations come in many forms. Among these are the methods used in computing EWs (and those used to determine continuum levels); the choice of atmospheric models including assumption of Local Thermodynamic Equilibrium (LTE)/non-LTE calculations and convective overshooting; the synthetic spectrum codes used; and the solar abundance values used to compute relative abundances, to name just a few. In general, an individual study will use identical techniques and parameters relating to these factors in order to maintain internal consistency. As such, we do not believe that systematic effects significantly alter the intra-cluster distribution computed from our database from the "natural" one.

The story for *inter*-cluster comparison is much more complicated. Experience has shown that even with high quality high-resolution data, the latest models and codes and very careful analysis, slight differences in approach between studies can yield significantly different results. Assuming an "intrinsic" inter-cluster η_C with some variance and mean δ_C, introducing systematics will cause a broadening and a shift in the mean. Searching for an estimate of the intrinsic distribution, such that adding a systematic treatment will result in an adequate representation of the data, is unrealistic given the complexity of inter-cluster pairs in the database. Systematics, for these purposes, should only affect pairs made from different literature sources. The differing number of clusters and stars per literature source also makes any simplified treatment impossible. To gauge the magnitude of both systematic effects, the mean shift and broadening, for the specific case of our database, we induce uncertainties in the data and extrapolate backward to a best guess of the intrinsic distribution.

To accomplish this a Monte-Carlo type of approach was taken, where in each simulation iteration, we added randomly derived uncertainties to the abundances of similar elements for all unique sources. In other words, the same random value was added to all the measurements of a given chemical species in a given literature study, regardless of cluster membership. The absolute values of our randomly derived uncertainties were taken from a Gaussian distribution whose parameters fit the distribution of uncertainties recorded in the database. Figure 2 shows both the literature uncertainties and our Gaussian model, which provides a reasonable fit to the data. The inter-cluster η_C is then computed from this set of simulated cluster abundances and can be compared to the true inter-cluster η_C from our database.

We computed 1000 iterations of the systematics simulation described above and derived η_C across all simulations. The resultant distribution is shown in the left panel of Figure 3 (grey), along with the data (blue), which have been shifted to align the peaks. The broadening due to simulated abundance uncertainties is evident. To reverse this process, or de-broaden, the difference between simulation and data is removed from the data to arrive at the green his-
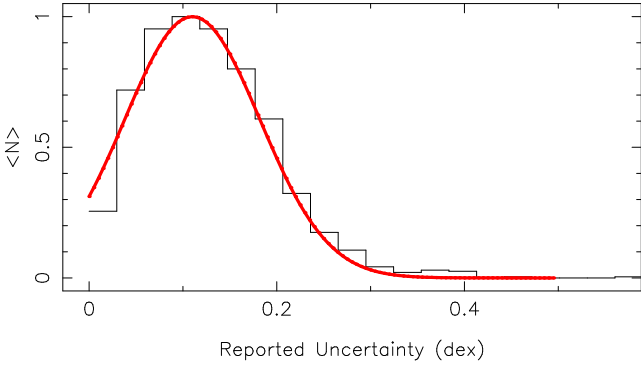
Figure 2. Gaussian fit (red) to the normalized distribution of uncertainties reported in the literature (black histogram).

togram in Figure 3, left panel. The grey cross-hatching illustrates the total change between simulations, data and the de-broadened distribution. Addition of the simulated uncertainties caused the mean δ_C in the resultant distribution to be shifted to a δ_C 56% larger than that of the original distribution. When corrected for the de-broadened distribution, in order to arrive at an estimate of the intrinsic distribution, we find the δ_C for which a 56% increase arrives at the data mean, this results in a peak at δ_C of $\sim$0.077 dex shown in the center panel of Figure 3, which is a repeat of Figure 1 using the "intrinsic" inter-cluster η_C instead of the data.

This is perhaps a crude approximation, but should nonetheless give an idea of the magnitude of potential effects. The uncertainties used, for example, are internal random errors computed in a variety of ways and may not represent the sources of error between studies as well. Specific considerations, however, are beyond the scope of this work. The bulk shift of our de-broadened distribution likely mis-represents the true rising edge. Specifically, the first two, perhaps three, bins shown in the center panel of Figure 3 are probably artefacts of this. Another artefact is visible in the simulated η_C in the left panel of Figure 3 at a δ_C of $\sim$0.05 dex. The origin of this feature is unclear, but, given its location, it does not affect our analysis in any meaningful way.

Internal, random, errors in abundance measurements will also alter the η_C distributions from their intrinsic profiles. Depending on the overlap between clusters in $\mathcal{C}$-space, the magnitude of this effect will be different for either population; however, the scatter induced in the intra-cluster population requires that its magnitude be greater. This implies that the overlap between η_C distributions seen in Figure 3, is an absolute upper limit, and the peaks would be separated by a greater distance in δ_C, favoring the distinction of clusters. The specific impact that systematic effects, as discussed here, have on our conclusions in this work will be discussed in further detail in the next section.

4   THE CLUSTER PROBABILITY FUNCTION

A major goal of this work is to derive a quantitative assessment of the ability to distinguish coeval stars from those born in distinct environments, based solely on their chemical signatures. The level of homogeneity that is expected within a Galactic open cluster, and the sparseness of the chemical space between them, are readily inferred from Figure 1. We now combine these two concepts to achieve this goal. The probability that a particular pair of stars are members of the same cluster based on their δ_C is related to the relative contributions of each η_C distribution, and can be expressed as
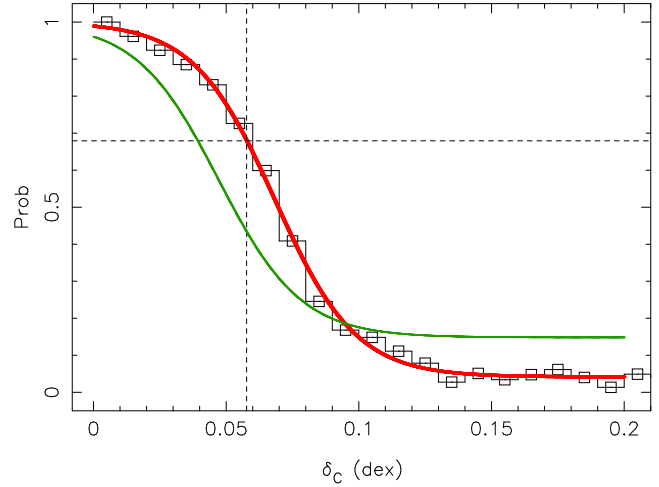

Figure 4. The intra-cluster probability function. The black squares and histogram show the discrete probability function for the same η_C distributions shown in Figure 1. The solid red line shows the least squares fit to this using the continuous function with parameters listed in Table 4, where the dashed cross-hairs represent the 68% confidence limit that a pair of stars are coeval. Shown in green is the continuous fit for the "intrinsic" inter-cluster η_C derived from our systematics considerations.

$$P_{\delta_C} \equiv prob(\delta_C) = \frac{\eta_C^{intra}}{\eta_C^{inter} + \eta_C^{intra}}$$

When computed for the specific η_C distributions plotted in Figure 1, we obtain the discrete probability function shown in Figure 4, where the cross-hairs represent the 68% confidence limit. Note the steepness of the function; by the time it reaches a δ_C of 0.1 dex, there is only approximately a 10-20% probability that those two stars are members of the same cluster. This places tight constraints on the performance of a chemical tagging survey (e.g. see Section 6).

4.1   A functional form of P_{δ_C}

We now seek a functional form to express the intra-cluster probability continuously as a function of δ_C. A modified form of the sigmoid function with four free parameters describes the data well and can be written as

$$prob(\delta_C) = c + \frac{1-c}{1 + ae^{b\delta_C - d}}$$

The c term accounts for the lower probability limit caused by the tail in the intra-cluster distribution, while the $1 - c$ term ensures that we do not obtain a probability greater than 1. The solid red line in Figure 4 shows the least squares best fit to the discrete probability function. The goodness of fit illustrates both the smooth nature of the η_C distributions, and the appropriateness of the continuous probability function.

Also shown in Figure 4 is a fit to the probability function from our derived "intrinsic" inter-cluster η_C (see Section 3). This fit (shown in the right panel of Figure 3, along with its discrete counterpart) assumed that the first bin, corresponding to a δ_C of zero, or identical chemistries, actually approaches one. Likewise, the second bin was ignored, both of these under the assumption that they are noise features arising from our crude systematics treatment.

The magnitude of possible systematic effects is quite visible. At the 68% confidence level the difference between the two functions is $\sim$0.015 dex. It is difficult to judge whether our "intrinsic"
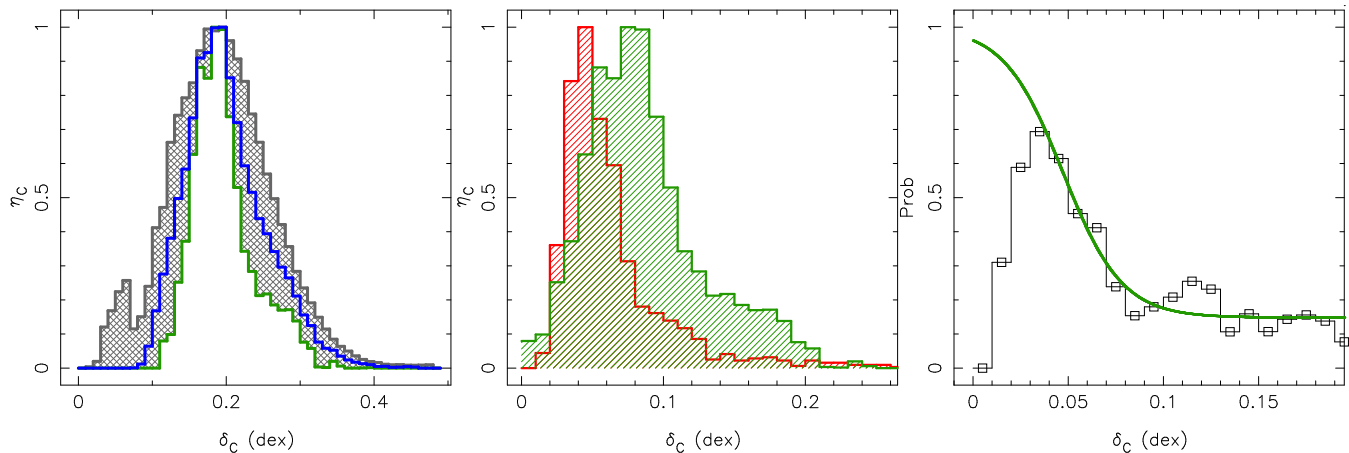
Figure 3. Summary of simulated inter-cluster systematics treatment. The left panel shows the η_C from 1000 systematics simulations (grey line), along with the peak-shifted data (blue) and the de-broadened and normalized "intrinsic" distribution (green). The center panel shows the "intrinsic" distribution peak-shifted to smaller δ_C based on the shift from our simulations. The rightmost panel shows the probability function (see Section 4) derived from the "intrinsic" η_C, and fit assuming the first two bins are an artefact of this crude treatment.

Table 4. Best fit parameters for P_{δ_C}

Parameter	Data	Systematics simulation
a	13.37	9.164
b	65.51	64.41
c	0.041	0.148
d	7.060	5.242

function actually represents such, but Figure 4 does help to illustrate the advantages of homogeneous abundance analysis, even if only to avoid the need for such considerations as applied here. The four parameters corresponding to each fit are listed in Table 4.

This formulation now provides us with a way of not only filtering the results of cluster finding algorithms, but importantly, a means to report the confidence with which we detect them. There will be a rate of attrition due to the overlap in the respective distributions, an effect which is likely due to natural scatter in addition to complex and not well understood processes occurring in the progenitors of all open clusters. We stress the importance of arriving at this probability function through empirical analysis of observational data. Until we can be confident that we fully understand all of the intricacies of star formation and Galactic chemical evolution, this empirical approach will remain the *only* way to achieve this.

This is not to say that the parameters listed in Table 4 are not subject to change. These most likely represent a lower limit to the ability to chemically tag, due to the heterogeneous analysis methods present in our abundance database. In the case of a large scale chemical abundance survey such as GALAH, or Gaia-ESO, a probability function specific to the analysis methods of that survey would be derived - so long as an appropriate calibration program targeting a number of established coeval populations were adopted. The analysis described in the present paper would be repeated using cluster abundance data from that calibration program. The Gaia-ESO survey serendipitously has this calibration built into its design, since it aims to target 100 Galactic open clusters. Possibly, though not ideally, this could serve as calibration for GALAH. For heterogeneous chemical tagging experiments (without the benefits of a uniform abundance analysis), the most up-to-date abundance data would be added to the literature abundance database and a new

probability function derived. In such a way, the function parameters could be iteratively improved. In the meantime, the function with parameters listed in Table 4 represent our current best guess, within the limitations of the abundance data in our database.

5   EXPLORATIONS IN $\mathcal{C}$-SPACE

Up to this point, all our discussion has been involving the η_C distributions whose δ_C metric computations were required to have at least a dimensionality of eight (i.e., a minimum of eight distinct elements being compared). This is not an entirely arbitrary decision, but one that is based both on the practicality of future chemical tagging experiments, and a delicate balance between optimising the cluster probability function and maintaining the statistical significance of the distributions themselves.

Bland-Hawthorn & Freeman (2004) estimated the minimum number of dimensions required to reveal a fraction of the approximately 10^8 clusters believed to be dissolved in the Galaxy. This figure, between 10-15 elements, has been incorporated into the design of the HERMES instrument for the purpose of the GALAH chemical tagging survey. Ting et al. (2012) confirm this number finding approximately 9 independently varying elements from the available abundance data. The constraint employed here matches well these capabilities, in fact, the mean number of elements in the intra- and inter-cluster η_C distributions came out to be 11 and 9, respectively. In other words, out of the total number of δ_C pairs in each distribution, half were computed with greater than, or equal to, 11 and 9 compatible element abundances. It is important, also, to understand the species that dominate each of the distributions. These will be the minimum set of species required to utilize the cluster probability function with the parameters listed in Table 4. In Figure 5, we plot the number of δ_C computations, per element, for both inter- and intra-cluster η_C. The 9 and 11 key elements for those two can clearly be seen in the upper portion of Figure 5; these are dominated by the α and Fe-peak elements, in addition to Ba, due to their relative ease of measurement. We stress that these do not necessarily represent the best chemical tagging discriminators, but rather that the high ranking elements shown are capable of chemical tagging at the level depicted in Figure 4, based on the data available.
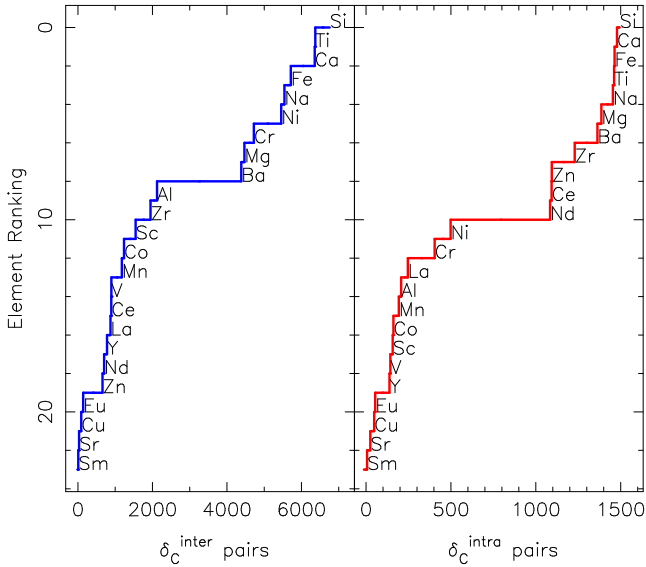
Figure 5. The numbers of δ_C computations making up each distribution shown in Figure 1. The "ranking" increases from top to bottom, where a lower number rank indicates greater significance in the overall distribution. This is *not* a reflection of the significance of any individual element as a chemical tagging probe, but rather informs the groups of elements generally necessary to utilise the cluster probability function described here.

Figure 6. The effects of dimensionality on the probability function. The top panel shows discrete and fit continuous probability functions for both the minimum 8 dimensions (upper;red) and no limit (lower;blue dotted) η_C distributions. The bottom panel shows residuals computed from $P^8_{\delta_C} - P^{all}_{\delta_C}$ for data (black histogram) and continuous representations (red line). The strongly positive residuals toward the intra-cluster portion (left-hand side) of the plot clearly speak to the necessity of a larger number of dimensions. Cross-hairs are as in Figure 4.

5.1 Probing chemical dimensionality

The role of dimensionality on chemical tagging can be tested using the formulation presented here. By relaxing the requirement that a minimum number of species be present in each δ_C computation we can include the entire database summarized in Table 1, which results in a minimum of 2 and mean of 5.6 dimensions. Figure 6 shows the probability functions derived from their η_C distributions, including continuous fits, and the residuals (both discrete and continuous) obtained by the difference $P^8_{\delta_C} - P^{all}_{\delta_C}$. It is evident from the excess in residuals at low δ_C that the reduction in dimensions results in a significant loss in the ability to perform chemical tagging. Our ability to explore the same effects for higher dimensions is trumped by the limited sample of studies with a wide range of element abundances. The sharp edge seen in both panels of Figure 5 (at rank 8 and 10 in left and right panels, respectively) illustrates this. The numbers of pairs dramatically reduce and noise immediately dominates our distributions. For example, with a minimum of 10 dimensions imposed, the number of inter-cluster pairs reduces by 80% and the number of clusters being probed cuts almost in half, from 27 to 14.

Although it is fairly intuitive at this point to conclude that increases in chemical dimensionality lead to improvements in the probability function, it must be noted that improvements, if any, would not necessarily be linear or predictable. The difficulty in deriving abundances for some elements (e.g., weak lines, few lines for EWs, etc.) at a given resolution could yield greater uncertainties and potential scatter, resulting in little improvement. Indeed, the limitations on probing higher dimensions in our literature abundance database likely are a result of this. Furthermore, elements whose abundance trends are coupled (e.g., see next section) would not singularly lend a comparable improvement over individual uncoupled elements.
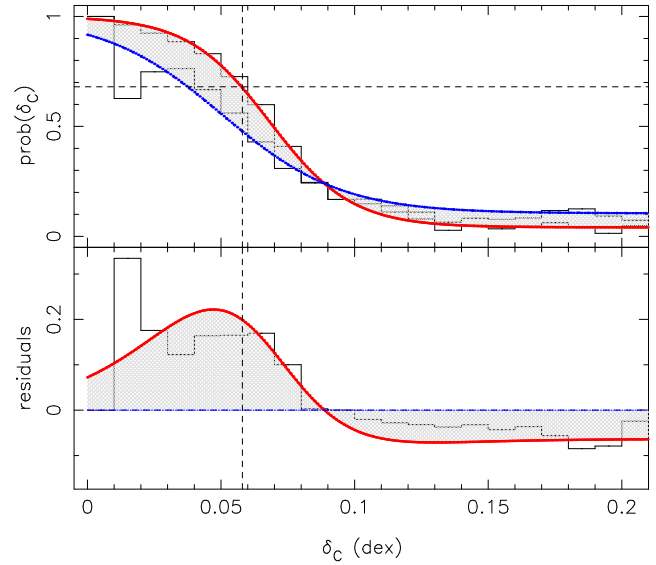
5.2 Probing specific elements

It is now clear that a number of chemical dimensions is required to differentiate clusters in the Galaxy. Each dimension, however, defined by the efficiency of its nucleosynthesis in the previous generation of stars, need not contribute evenly to the overall distribution. Elements whose processes are relatively insensitive to stellar mass, for instance, will be generated in most cases and the amount may only depend on a few parameters of the progenitor cloud. We explore the role of individual species in the probability function by recomputing the δ_C metric for each pair, *ignoring* that species. The probability function computed from the resulting distributions is then compared to that from the originals. Figure 7 shows the residuals obtained by subtracting the new function from that depicted in Figure 4 (red line) and Table 4, for a range of elements with a high ranking (as from Figure 5). Each panel also plots a linear regression to the residuals in the range from 0 to 0.25 (beyond this range the functions become extremely noisy and mostly meaningless), in order to illustrate the general trends. In these plots, a positive residual can be interpreted to imply that the element in question contributes above average to cluster differentiation, i.e., abundance homogeneity is preserved within a cluster while the abundance dispersion between clusters is increased for that element. This is particularly true at the low end of the δ_C spectrum (i.e. intra-cluster probability greater than approximately the 68% level) where chemical tagging is possible, marked by the vertical dashed line in Figure 7.

Typically, for the α and Fe peak elements probed, the level of influence is average to within the noise, at less than about 1-2%. This is not to say that they are poor chemical tagging elements, only that they act in concert, providing the robustness and noise reduction of greater numbers of dimensions. The α panel of Figure 7 exemplifies this point, where here the combination of Na, Mg, Al, Si and Ca acts as a proxy for the α elements. Although the resultant
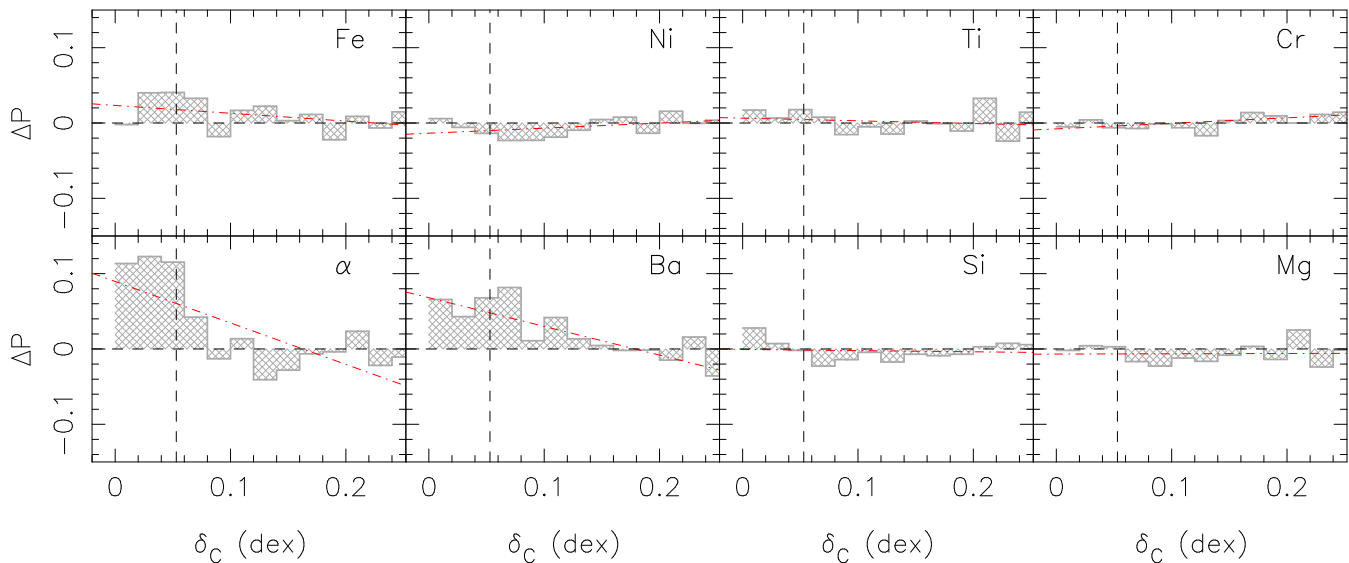
Figure 7. Examining the role of chemical tagging species in the cluster probability function. Each panel shows the difference residuals between the function derived in the text and one derived with the particular element, as indicated, ignored in the δ_C metric computation. For most of the elements listed, the effect is quite small and generally linear. The negative slope, and positive residuals residuals in the low end of the plot without Ba, indicates its power as a chemical tagging discriminator.

η_C must suffer from an increase in noise due to diminishing numbers of dimensions (the total number of pairs is still preserved), it is quite clear that the effect on the cluster probability is significant, at greater than the 10% level throughout intra-cluster regime.

Fe and Si seem to be exceptions, contributing closer to the 3-4% level on their own. The heavy n-capture element Ba single-handedly alters the cluster probability by close to 8%. Ba can be produced both through the slow and rapid n-capture processes, in low mass AGB (e.g. Busso et al. 2001) and core-collapse supernovae (e.g. Kratz et al. 2007), respectively, giving a wide range of conditions owing to the observed scatter in disk field and between Galactic open clusters (D'Orazi et al., 2009; Bensby et al., 2005). The dependence on age found by D'Orazi et al. (2009) may also be related to its power as a cluster discriminator. Different clusters evolving on different time-spans will exhibit distinct efficiencies in Ba production, which are then imprinted on the new forming cluster stars. These possibilities imply that other elements, such as La, Nd and Eu, that form through similar processes, may lend to a significant improvement to the P_{δ_C}; however, due to the limited availability of their abundances in the literature our sample does not contain sufficient numbers to explore these effects further. We must not discount that non-LTE effects, which may lead to significant overestimate of Ba abundances in young stars, could be responsible for some of its perceived power.

There are many factors conspiring to make meaningful comparisons for other elements difficult, not least of which is the stark drop off in numbers of pairs for elements beyond those in Figure 7. Provided that there are proper calibrations against known Galactic open clusters, upcoming large scale abundance surveys, such as GAL AH, will be highly optimised for these types of investigations.

6 CLUSTER RECONSTRUCTION

6.1 Mock chemical tagging experiment

We have already touched on the fact that the overlap between the intra- and inter-cluster η_C implies that clustering detection efficiency can not be 100%. In order to maximise the confidence with which we report detections, we must sacrifice potential members in lieu of including non-members. The actual efficiency which can be achieved is a function of the area of the overlapping regions between intra- and inter-cluster η_C (see Figure 1), and the confidence limit, P_{lim}, set on detections (e.g. 68, 90, 98%). In order to establish how said overlap affects the recovery of clusters, and to demonstrate a practical application of the probability function to a group of cluster candidates, we have performed a blind chemical tagging experiment using the abundance database discussed herein. A brief description of the method used follows.

δ_C was computed for each distinct pair of stars, ignoring our *a-priori* knowledge of cluster membership, thus emulating a true chemical tagging survey. We then identified all pairs with a probability P_{δ_C} greater than P_{lim}, where P_{lim} was evaluated at 68, 85, and 90%. Starting with the most significant pair of this subset, stars were added to groups where all pairs in the resulting group have at most a δ_C corresponding to P_{lim}. After addition to a group, a star was removed from the subset of significant pairs. When no more stars could be added to the current group, the next most significant pair was identified and this process repeated. Grouping was then completed when all pairs of the subset were exhausted. In this method *all* pairs of members of a candidate group have at most δ_C corresponding to P_{lim}, as opposed to the group mean. This restriction ensures we identify the core of a cluster and limits the runaway in linkages that would otherwise occur. This is not particularly sophisticated, and there may be more optimal methods such as evolving the cluster mean as members get added, but it does ensure a strict and invariant interpretation of P_{lim} for our simple experiment.

Table 5 summarizes the results of our experiment for P_{lim} of

Table 5. Summary of chemical tagging test experiments

P_{lim}	N	Detection Rate	Contamination Rate	Fragmentation Rate	Mean N_{detect}	Mean efficiency
68	16	59%	50%	25%	7.50	42%
85	20	74%	50%	50%	4.85	25%
90	9	33%	22%	57%	4.67	19%

68, 85 and 90%. Here, our definition of a cluster requires at least three members (e.g., a single high significance pair would not be considered a cluster), and a "clean" detection is defined as one where all recovered group members reside in the same true cluster (but do not necessarily comprise the whole true cluster). A brief description of the columns of Table 5 follows. N gives the number of clusters detected in total, the Detection Rate compares N to the number of true clusters in the experiment, which is 27. The Contamination Rate is a measure of the overall quality of detections and is the fraction of all detections with members from more than a single true cluster (e.g. not a clean detection). The Fragmentation Rate is the fraction of clean detections that are repeats, a high value of which represents an over-sensitivity to internal cluster scatter. For example, the 57% fragmentation rate in $P_{lim} = 90$ comes from the fact that out of the 7 clean detections, 5 were made from stars of the same Hyades study, making 4 repeats. N_{detect} is simply the mean number of stars in each group, while the mean efficiency measures the recovery rate of clean clusters, computed as the number of detected members divided by the total number of true members.

6.2 Efficiency and constraints

Table 5 illustrates some of the challenges of chemical tagging and gives an idea of what to expect in terms of efficiency and contamination. It should be noted, however, that the efficiency tabulated may not be particularly faithful to a true experiment. Many of the literature studies have low numbers of stars, while the Hyades sample of De Silva et al. (2006) and Paulson et al. (2003) contains 46 members. The stark contrast with little middle ground implies that our numbers likely represent upper bounds, since few clusters would be expected to have only several members, although it is unclear how Galactic dynamical effects, such as disk mixing, spiral scatter, and radial migration would affect the number of original cluster members expected to be in the scope of a chemical tagging survey. The fragmentation rate is also dominated by the Hyades, primarily due to our requirement of at least three candidate members per detection, and may represent a lower bound.

It is important to understand that the efficiency tabulated in Table 5 does not represent the total efficiency of recovering clusters, but rather the per detection efficiency of recovering members of a cluster. The total chemical tagging cluster detection efficiency is related to at least the detection rate, contamination rate, fragmentation rate, and mean efficiency combined. A simple calculation for the $P_{lim} = 90$ case gives a total efficiency of ~2% (0.33*(1-0.22)*(1-0.57)*0.19*100%). This is an efficiency of placing individual stars in their birth clusters; the efficiency of detecting any fossil of an existing association would ignore the mean efficiency column and hence for $P_{lim} = 90$ evaluates to ~12%. In a million star survey we might then expect to place 20,000 stars in associations. Given the mean N_{detect} of 4.67, this would amount to approximately 4300 clusters being recovered in such a survey, to the 90% confidence level.

Of course, this is a preliminary number using the literature abundance database, as are all numbers listed in Table 5; a more realistic approximation would only be possible using the P_{δ_C} calculated from a GALAH calibration program as described in Section 4.1. It is also important to note that there is an implicit assumption in this calculation that all stars were indeed born in clusters similar to those that we observe today. Bland-Hawthorn et al. (2010a) suggest, based on their chemical evolution models, that clusters in the low metallicity regime, corresponding to early generations of star formation, are more clumped in chemical space, with a wider range of abundance variation between clusters. This would certainly result in a different probability function, leading to higher chemical tagging efficiencies, since the literature abundance database used here is restricted to higher metallicities ($> \sim \ -0.35$ dex), due to the metallicity distribution of Galactic open clusters. However, since most stars in the Galactic disk are also in the higher metallicity range, this effect may not be important for most chemical tagging experiments.

6.3 Tools for chemical tagging

The methods used in these mock experiments are not a recommendation of how to perform group finding on large data-sets. The requirement of computing the pair-wise δ_C metric over thousands, or millions, of stars may not be the most efficient way to identify structure. They do, however, suggest an algorithm for validating and verifying a group of potential coeval stars, G, identified within a larger sample of stars (e.g. a Galactic disk field sample) via any means:

1.) Compute δ_C between all pairs of group G.
2.) Identify the δ_C value, δ_C^{lim}, corresponding to desired P_{lim} from P_{δ_C}.
3.) Identify all pairs where $\delta_C \leq \delta_C^{lim}$.
4.) All stars making up the pairs from 3.) are set S_c
5.) All stars making up the pairs *not* included in 3.) are set S_{nc}
6.) G is re-evaluated to be the complement of S_{nc} in S_c.
7.) Finally, the cluster detection confidence, P_{clus}, is evaluated using the mean of δ_C in G.

Aside from ensuring that all pairs in the resultant group have a high probability of being natal siblings, following the preceding prescription yields a qualitative assessment of our confidence in the cluster detection based on a global knowledge of the chemical nature of Galactic open clusters.

Figure 8 is a graphical representation of the above pipeline, for clarity. The overlap in the sets S_{nc} and S_c illustrates the stars that comprise both high and low probability pairs. Only the stars inside the shaded region of S_c are then included as members in the final cluster detection. The final number of δ_C pairs shown at the bottom of the pipeline will be less than the number of confident pairs (those having $P \geq P_{lim}$) shown above, if there is overlap between S_{nc} and S_c as depicted in this diagram.

This pipeline can be run efficiently, without the need for computing the δ_C metric over all pairs, with the density based
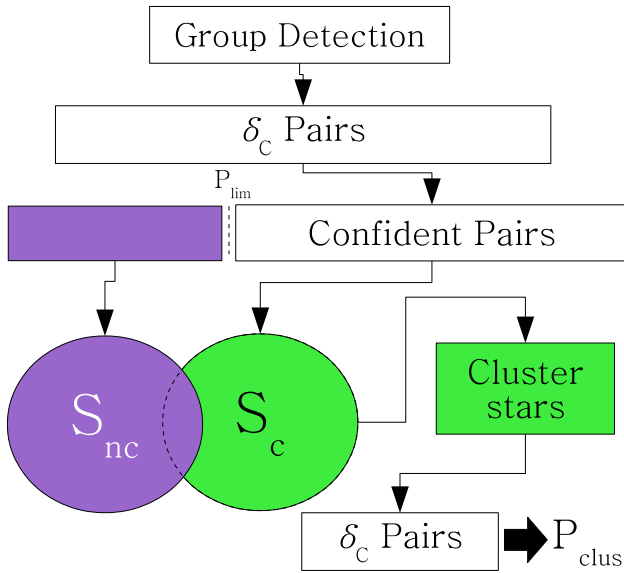
Figure 8. Flow diagram describing the steps outlined in section 6.3 for validation and verification of cluster finding via chemical tagging. The overlap shown between S_{nc} and S_c represents the stars that are in both confident and non-confident δ_C pairs. Only those in confident and *not* in non-confident (i.e. the green region of the S_c circle) comprise the final cluster members.

group finding algorithm, **EnLink**, described in Sharma & Johnston (2009). The final cluster stars derived from the set S_c shown in Figure 8, would result from a δ_C cut in the group detections output by EnLink. A further investigation of this application, and the overall use of P_{δ_C}, is forthcoming based on a fully blind chemical tagging experiment on a homogeneous abundance dataset of several hundred thin and thick disk field stars.

7 SUMMARY & CONCLUSIONS

We have introduced a metric, the δ_C metric, designed to quantify the chemical difference of a pair of stars in a single context, regardless of the number or nature of the measured element abundances, between distinct pairs. Using a database constructed from high-resolution literature abundance studies of Galactic open clusters, we have analyzed the relative contributions of δ_C pairs for both intra- and inter-cluster pairs, to arrive at a probability function, P_{δ_C}, describing the likelihood that two stars share the same evolutionary origin.

For the specific case of a minimum of 8 chemical dimensions, we have derived parameters to a functional form of P_{δ_C}, whose 68% confidence level (analogous to a 1-σ detection) lies at a δ_C of ~0.058 dex. This level, in addition to the steep slope present in P_{δ_C}, informs the accuracy necessary to distinguish cluster members from polluting stars. We have probed the effect of variations in the dimensionality of chemical space and the role of individual elemental species on the probability function. It is clear that limiting the number of dimensions present severely reduces the inter-cluster variations, and thus the approximately nine species prevalent in our analysis are a minimum recommendation. Unfortunately, owing to the difficulty of measurement, we could not explore higher dimensions. Of the key players, the α elements (by proxy), Fe and Ba particularly stand out, contributing up to 10% of the P_{δ_C} each.

We have placed these results in the context of chemical tag-

ging, and shown how they can be used to validate and verify coeval groups discovered via any means. An important outcome is the ability to determine and report a confidence of detection, based on our observational understanding of Galactic structure as opposed to theoretical models or arbitrary statistical tests. We have utilized this ability to highlight some of the challenges involved in a true chemical tagging experiment. It is evident that the reconstruction of coeval groups of stars, dispersed open clusters, via the technique of chemical tagging is a difficult, but plausible, venture. Even though it is impossible to reconstruct all such groups, and seems unlikely even to discover *most*, the numbers in Table 5 point to valuable information that can be inferred about what cannot be detected, from what can. They also speak to the advantages of a very large sample of data, given the low efficiencies even at low confidence levels.

The requirements for internal abundance accuracy of a chemical tagging survey such as GALAH can be gleaned from the intra-cluster probability function. However, this function has been derived from the currently available set of abundance data in the literature which matched our requirements for resolution, elements, and number of stars, analysed in several different ways between literature studies. With such a heterogeneous sample, considerations of systematics effects must not be ignored, and may result in significant performance loss as discussed in Sections 3 and 4. The function derived in this analysis is only the best guess to date and its use requires understanding the caveats discussed in this text. The results, however, show that the methods introduced here provide a powerful tool for conducting and understanding chemical tagging in a practical sense. To achieve the best possible confidence in cluster reconstruction, a chemical tagging experiment of large scale should calibrate against a number of known clusters in order to derive P_{δ_C} for the specific analysis methods used therein.

Finally, a pipeline recipe for validation and verification of coeval groups of stars detected using element abundances only, has been developed. A logical next step is to use this recipe in a small scale chemical tagging experiment to further develop these methods in a real world scenario, and to demonstrate how the tool En-Link can be applied to this problem. Such an experiment is currently in progress by the authors on a large homogeneous sample (several hundreds) of stars with a wide range of high-resolution abundance measurements.

References

Barden, S. C., Jones, D. J., Barnes, S. I., et al. 2010, in Society of Photo-Optical Instrumentation Engineers (SPIE) Conference Series, Vol. 7735, Society of Photo-Optical Instrumentation Engineers (SPIE) Conference Series, 9–19

Batista, S. F. A., & Fernandes, J. 2012, New A, 17, 514

Bensby, T., Feltzing, S., Lundström, I., & Ilyin, I. 2005, A&A, 433, 185

Bland-Hawthorn, J., & Freeman, K. C. 2004, PASA, 21, 110

Bland-Hawthorn, J., Karlsson, T., Sharma, S., Krumholz, M., & Silk, J. 2010a, ApJ, 721, 582

Bland-Hawthorn, J., Krumholz, M. R., & Freeman, K. 2010b, ApJ, 713, 166

Bragaglia, A., Sestito, P., Villanova, S., et al. 2008, A&A, 480, 79

Bubar, E. J., & King, J. R. 2010, AJ, 140, 293

Busso, M., Gallino, R., Lambert, D. L., Travaglio, C., & Smith, V. V. 2001, ApJ, 557, 802

Busso, M., Gallino, R., & Wasserburg, G. J. 1999, ARA&A, 37, 239

Carrera, R., & Pancino, E. 2011, A&A, 535, A30

Carretta, E., Bragaglia, A., & Gratton, R. G. 2007, A&A, 473, 129

Carretta, E., Bragaglia, A., Gratton, R. G., Lucatello, S., & D'Orazi, V. 2012, ApJ, 750, L14

Carretta, E., Bragaglia, A., Gratton, R. G., & Tosi, M. 2005, A&A, 441, 131

De Silva, G. M., Freeman, K. C., Asplund, M., et al. 2007a, AJ, 133, 1161

De Silva, G. M., Freeman, K. C., Bland-Hawthorn, J., Asplund, M., & Bessell, M. S. 2007b, AJ, 133, 694

De Silva, G. M., Freeman, K. C., Bland-Hawthorn, J., et al. 2011, MNRAS, 415, 563

De Silva, G. M., Gibson, B. K., Lattanzio, J., & Asplund, M. 2009, A&A, 500, L25

De Silva, G. M., Sneden, C., Paulson, D. B., et al. 2006, AJ, 131, 455

D'Orazi, V., Magrini, L., Randich, S., et al. 2009, ApJ, 693, L31

D'Orazi, V., & Randich, S. 2009, A&A, 501, 553

Eggen, O. J. 1994, in Galactic and Solar System Optical Astrometry, ed. L. V. Morrison & G. F. Gilmore, 191

Ford, A., Jeffries, R. D., & Smalley, B. 2005, MNRAS, 364, 272

Freeman, K., & Bland-Hawthorn, J. 2002, ARA&A, 40, 487

Friel, E. D. 1995, ARA&A, 33, 381

Gebran, M., & Monier, R. 2008, A&A, 483, 567

Gebran, M., Monier, R., & Richard, O. 2008, A&A, 479, 189

Gilmore, G., Randich, S., Asplund, M., et al. 2012, The Messenger, 147, 25

Gonzalez, G., & Wallerstein, G. 2000, PASP, 112, 1081

Iben, J. 1967, ApJ, 147, 624

Janes, K. A., & Phelps, R. L. 1994, AJ, 108, 1773

Janes, K. A., Tilley, C., & Lynga, G. 1988, AJ, 95, 771

Kaluzny, J., & Rucinski, S. M. 1995, A&AS, 114, 1

Karakas, A., & Lattanzio, J. C. 2007, PASA, 24, 103

Kratz, K.-L., Farouqi, K., Pfeiffer, B., et al. 2007, ApJ, 662, 39

Lada, C. J., & Lada, E. A. 2003, ARA&A, 41, 57

Magrini, L., Randich, S., Zoccali, M., et al. 2010, A&A, 523, A11

Mitschang, A. W., De Silva, G. M., & Zucker, D. B. 2012, MNRAS, 422, 3527

Montes, D., López-Santiago, J., Gálvez, M. C., et al. 2001, MNRAS, 328, 45

Pace, G., Pasquini, L., & François, P. 2008, A&A, 489, 403

Paulson, D. B., Sneden, C., & Cochran, W. D. 2003, AJ, 125, 3185

Pereira, C. B., & Quireza, C. 2010, in IAU Symposium, Vol. 266, IAU Symposium, ed. R. de Grijs & J. R. D. Lépine, 495–498

Phelps, R. L., Janes, K. A., & Montgomery, K. A. 1994, AJ, 107, 1079

Pompéia, L., Masseron, T., Famaey, B., et al. 2011, MNRAS, 415, 1138

Randich, S., Sestito, P., Primas, F., Pallavicini, R., & Pasquini, L. 2006, A&A, 450, 557

Reddy, A. B. S., Giridhar, S., & Lambert, D. L. 2012, MNRAS, 419, 1350

Sestito, P., Bragaglia, A., Randich, S., et al. 2008, A&A, 488, 943

Sharma, S., & Johnston, K. V. 2009, ApJ, 703, 1061

Shen, Z.-X., Jones, B., Lin, D. N. C., Liu, X.-W., & Li, S.-L. 2005, ApJ, 635, 608

Shu, F. H., Adams, F. C., & Lizano, S. 1987, ARA&A, 25, 23

Smiljanic, R., Gauderon, R., North, P., et al. 2009, A&A, 502, 267

Soderblom, D. R., Laskar, T., Valenti, J. A., Stauffer, J. R., & Rebull, L. M. 2009, AJ, 138, 1292

Tabernero, H. M., Montes, D., & Gonzalez Hernandez, J. I. 2012, A&A, in press, ArXiv:1205.4879

Tautvaišiene, G., Edvardsson, B., Tuominen, I., & Ilyin, I. 2000, A&A, 360, 499

Ting, Y. S., Freeman, K. C., Kobayashi, C., de Silva, G. M., & Bland-Hawthorn, J. 2012, MNRAS, 421, 1231

Torres, C. A. O., Quast, G. R., Melo, C. H. F., & Sterzik, M. F. 2008, Young Nearby Loose Associations, ed. B. Reipurth, 757

Wallerstein, G., Iben, J., Parker, P., et al. 1997, Reviews of Modern Physics, 69, 995

Xin, Y., & Deng, L. 2005, ApJ, 619, 824

Zuckerman, B., & Song, I. 2004, ARA&A, 42, 685